The transcription factor ATF4 regulates glucose metabolism in mice through its expression in osteoblasts

Tatsuya Yoshizawa,[1] Eiichi Hinoi,[1] Dae Young Jung,[2] Daisuke Kajimura,[1] Mathieu Ferron,[1] Jin Seo,[3] Jonathan M. Graff,[3] Jason K. Kim,[2,4] and Gerard Karsenty[1]

[1]Department of Genetics and Development, Columbia University College of Physicians and Surgeons, New York, New York, USA. [2]Program in Molecular Medicine, University of Massachusetts Medical School, Worcester, Massachusetts, USA. [3]Department of Developmental Biology, University of Texas Southwestern Medical Center, Dallas, Texas, USA. [4]Department of Medicine, Division of Endocrinology, University of Massachusetts Medical School, Worcester, Massachusetts, USA.

The recent demonstration that osteoblasts have a role in controlling energy metabolism suggests that they express cell-specific regulatory genes involved in this process. Activating transcription factor 4 (ATF4) is a transcription factor that accumulates predominantly in osteoblasts, where it regulates virtually all functions linked to the maintenance of bone mass. Since *Atf4*$^{-/-}$ mice have smaller fat pads than littermate controls, we investigated whether ATF4 also influences energy metabolism. Here, we have shown, through analysis of *Atf4*$^{-/-}$ mice, that ATF4 inhibits insulin secretion and decreases insulin sensitivity in liver, fat, and muscle. Several lines of evidence indicated that this function of ATF4 occurred through its osteoblastic expression. First, insulin sensitivity is enhanced in the liver of *Atf4*$^{-/-}$ mice, but not in cultured hepatocytes from these mice. Second, mice overexpressing ATF4 in osteoblasts only [termed here α1(I)Collagen-Atf4 mice] displayed a decrease in insulin secretion and were insulin insensitive. Third, the α1(I)Collagen-Atf4 transgene corrected the energy metabolism phenotype of *Atf4*$^{-/-}$ mice. Fourth, and more definitely, mice lacking ATF4 only in osteoblasts presented the same metabolic abnormalities as *Atf4*$^{-/-}$ mice. Molecularly, ATF4 favored expression in osteoblasts of *Esp*, which encodes a product that decreases the bioactivity of osteocalcin, an osteoblast-specific secreted molecule that enhances secretion of and sensitivity to insulin. These results provide a transcriptional basis to the observation that osteoblasts fulfill endocrine functions and identify ATF4 as a regulator of most functions of osteoblasts.

Introduction

The transcriptional control of osteoblast differentiation and function involves many players, some broadly expressed and others with a more restricted expression (1). At least 3 of these transcription factors accumulate only or mostly in osteoblasts: Runx2, Osterix, and activating transcription factor 4 (ATF4) (2–5). The first 2 are critical determinants of the transition from mesenchymal cells to the osteoblast lineage. The third one, ATF4, a member of the cAMP-responsive element-binding protein (CREB) family of basic zipper-containing proteins, regulates terminal differentiation and virtually all functions of the osteoblast related to the control of bone mass. Indeed, through its ability to regulate amino acid import, ATF4 is a critical determinant of the synthesis of proteins such as type I collagen in osteoblasts (4–6). Since type I collagen is the most abundant protein of the bone ECM, ATF4 is de facto a regulator of bone formation and of bone ECM mineralization (7). Additionally, ATF4 favors expression in osteoblasts of *Rankl*, a gene required for osteoclast differentiation; thus, through its osteoblastic expression, it also promotes bone resorption (8, 9). That ATF4 regulates these osteoblast functions raises the hypothesis that it may be an even more global regulator of osteoblast biology.

Recently, it was shown that the osteoblast is an endocrine cell type that, through the secreted molecule osteocalcin, favors insulin secretion by β cells and insulin sensitivity in liver, muscle, and adipocytes (10–12). The function of osteocalcin is regulated by at least one regulatory gene expressed in osteoblasts called embryonic stem cell phosphatase (*Esp*). The *Esp* gene product inhibits indirectly the biological activity of osteocalcin by favoring its carboxylation (10). The notion that the osteoblast may be an endocrine cell type raises the prospect that osteoblasts must express other regulatory genes such as those encoding transcription factors that may be implicated in this aspect of its biology.

While studying *Atf4*$^{-/-}$ mice for another purpose, we were surprised to notice significantly lower fat mass and blood glucose levels. These observations echoed the glucose intolerance noted in humans lacking the eukaryotic translation initiation factor 2 kinase (*EIF2AK3*), which enhances ATF4 translation during amino acid starvation or ER stress (13, 14). In addition, it is known that phosphorylation of eukaryotic translation initiation factor 2α (eIF2α) regulates glucose homeostasis (15–17). We show here that ATF4 is in fact a negative regulator of insulin secretion and of sensitivity to insulin in liver, muscle, and fat. Surprisingly, however, cell-based assays and analyses of classical and cell-specific loss-of-function and gain-of-function mouse models and of compound mutant mice reveal that ATF4 regulates glucose metabolism through its expression in osteoblasts. In these latter cells, ATF4 favors expression of *Esp* and as a result decreases the bioactivity of osteocalcin. This study reveals a further level of control of the endocrine function of osteoblasts and supports the notion that ATF4 regulates most functions of this cell type.

Authorship note: Tatsuya Yoshizawa and Eiichi Hinoi contributed equally to this work.

Conflict of interest: The authors have declared that no conflict of interest exists.

Citation for this article: *J. Clin. Invest.* **119**:2807–2817 (2009). doi:10.1172/JCI39366.

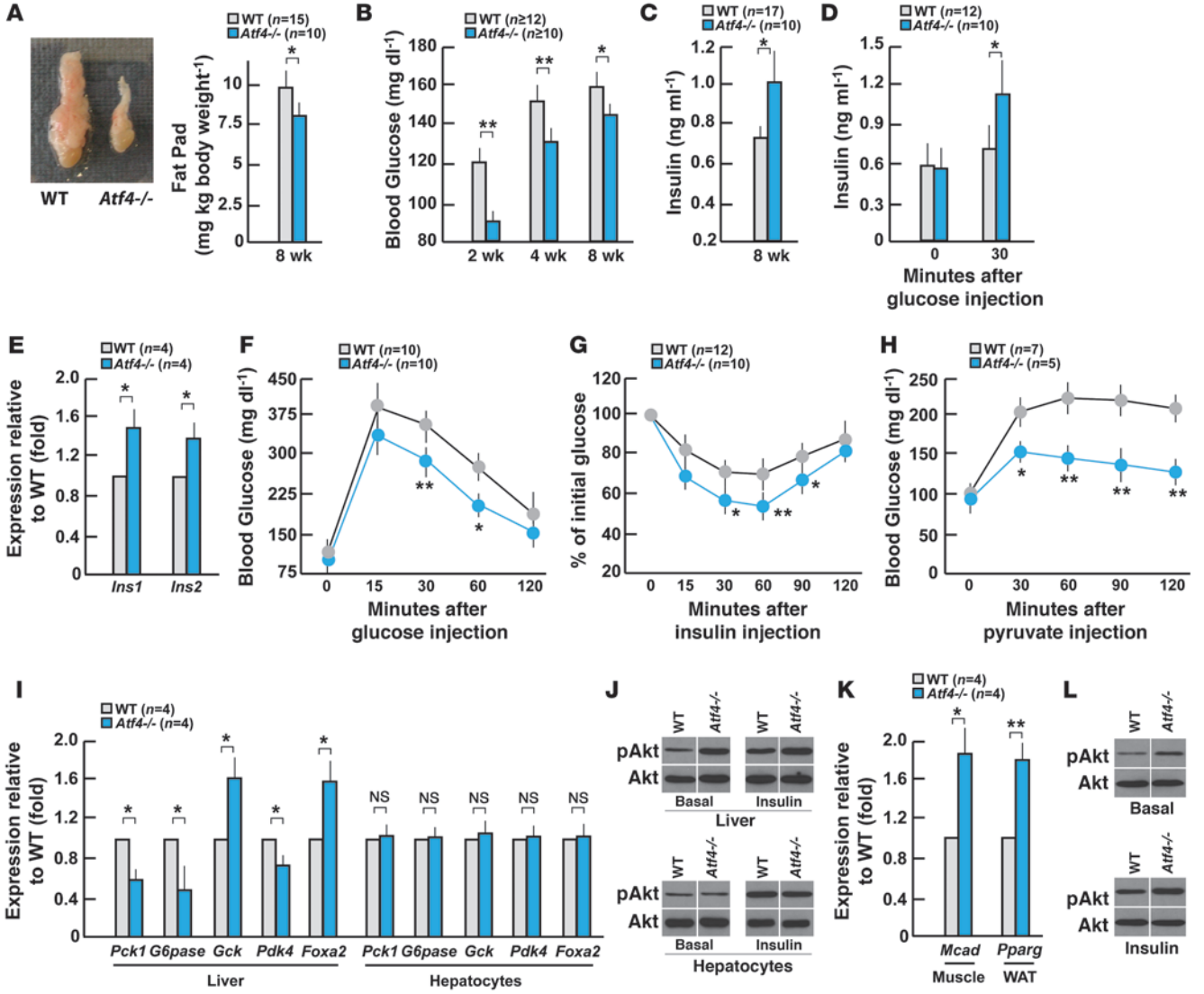

Figure 1

Atf4 inactivation increases glucose tolerance. (**A**) Photograph of representative fat pad (16 weeks of age) and histogram showing fat pad weight over body weight in WT and *Atf4*$^{-/-}$ mice. (**B** and **C**) Blood glucose and serum insulin levels in WT and *Atf4*$^{-/-}$ mice at indicated ages. (**D**) Results of GSIS test in WT and *Atf4*$^{-/-}$ mice. (**E**) *Insulin* expression in pancreas of WT and *Atf4*$^{-/-}$ mice. (**F**) GTT in WT and *Atf4*$^{-/-}$ mice. (**G** and **H**) ITT and PTT in WT and *Atf4*$^{-/-}$ mice. (**I**) Insulin target gene and insulin sensitivity marker gene expression in *Atf4*$^{-/-}$ liver or cultured hepatocytes. (**J**) Phosphorylation of Akt in *Atf4*$^{-/-}$ liver (upper panels) or cultured hepatocytes (lower panels) at basal and insulin-stimulated conditions. (**K**) Insulin sensitivity marker gene expression in muscle and white adipose tissue (WAT) in *Atf4*$^{-/-}$ mice. (**L**) Phosphorylation of Akt in muscle in *Atf4*$^{-/-}$ mice at basal (upper panel) and insulin-stimulated (lower panel) conditions. Analysis of 8-week-old *Atf4*$^{-/-}$ mice is shown in **D**–**L**. Images in **J** and **L** were grouped from different parts of the same gel and film. Error bars show mean + SEM. $^{**}P < 0.01$; $^{*}P < 0.05$, WT versus *Atf4*$^{-/-}$ mice.

Results

Atf4 inactivation enhances secretion of and sensitivity to insulin. While studying whether ATF4 could mediate the effect of serotonin on osteoblasts (18), we noticed that *Atf4*$^{-/-}$ mice had smaller fat pads than their WT counterparts (Figure 1A). This feature prompted us to analyze their energy metabolism.

The first abnormality that this study revealed was that *Atf4*$^{-/-}$ mice displayed at 2 weeks, 1 month, and 2 months of age a significant decrease in blood glucose levels when compared with WT littermates (Figure 1B). This decrease in blood glucose levels was secondary to an increase in circulating insulin levels, which itself was secondary to an increase in insulin secretion as determined by a glucose-stimulated insulin secretion (GSIS) test (Figure 1, C and D). The existence of these abnormalities led us to analyze histologically WT and *Atf4*$^{-/-}$ pancreata. β cell area and β cell proliferation were significantly increased as were *Insulin* (*Ins*) expression and insulin content in *Atf4*$^{-/-}$ compared with WT islets (Figure 1E and Table 1). The decrease in blood glucose levels in the face of an increase in circulating levels of insulin suggested that *Atf4*$^{-/-}$ mice were more tolerant to glucose than WT littermates. To demonstrate that this was the case, we performed glucose tolerance tests (GTT) via i.p. injection of glucose (2 g/kg of body weight) after overnight fasting. These tests showed that *Atf4*$^{-/-}$ mice were indeed significantly more tolerant to a glucose load than WT mice (Figure 1F).

Table 1
Insulin contents, β cell area, and quantification of insulin/Ki67-positive cells in WT and *Atf4*$^{-/-}$ mice

	WT ($n \geq 4$)	*Atf4*$^{-/-}$ ($n \geq 4$)
Insulin content (ng/mg pancreas)	126.2 ± 17.4	169.2 ± 22.1[A]
β cell area (%)	0.91 ± 0.17	1.24 ± 0.14[A]
Ki67-positive cells (%)	1.57 ± 0.28	2.16 ± 0.30[A]

[A]$P < 0.05$. Analysis is from 8-week-old *Atf4*$^{-/-}$ mice.

In principle, one would expect that an increase in insulin secretion would cause a decrease in insulin sensitivity in *Atf4*$^{-/-}$ mice. Remarkably, however, when we analyzed this aspect of glucose metabolism through an insulin tolerance test (ITT), we noticed that *Atf4*$^{-/-}$ mice were also more sensitive to insulin than WT littermates (Figure 1G). This increase in insulin sensitivity was next verified by molecular studies performed in various target organs of insulin (see below).

To determine whether gluconeogenesis, a process inhibited by insulin in the liver (19, 20), might be under the control of ATF4, we performed pyruvate tolerance tests (PTT) via i.p. injection of pyruvate (2 g/kg of body weight) in WT and *Atf4*$^{-/-}$ mice. *Atf4*$^{-/-}$ mice showed a marked reduction in glucose production after a pyruvate challenge compared with WT mice, indicating that gluconeogenesis was impaired by the absence of ATF4 (Figure 1H). To further show that gluconeogenesis is reduced in *Atf4*$^{-/-}$ mice, we analyzed the expression of phosphoenolpyruvate carboxykinase (*Pck1*) and glucose-6-phosphatase (*G6pase*), 2 well-known insulin target genes in the liver that are implicated in this process (21, 22). A significant reduction of the expression of both genes was detected in *Atf4*$^{-/-}$ mice (Figure 1I), further confirming the inhibition of hepatic gluconeogenesis in these animals. To determine whether glycolysis might be altered in *Atf4*$^{-/-}$ mice, we analyzed the expression of 2 key genes, glucokinase (*Gck*) and pyruvate dehydrogenase kinase 4 (*Pdk4*), involved in this process and whose expression is regulated by insulin in the liver (23, 24). In *Atf4*$^{-/-}$ mice, *Gck* expression was significantly increased, while *Pdk4* expression was significantly decreased (Figure 1I), indicating that glycolysis was stimulated by the absence of *Atf4*. Furthermore, the expression of the transcription factor *Foxa2*, which regulates insulin sensitivity (25), was also increased in the liver of *Atf4*$^{-/-}$ mice (Figure 1I). To further confirm that ATF4 regulates insulin signaling in liver in vivo, we studied phosphorylation of Akt and glycogen synthase kinase 3 β (GSK-3β), an event triggered by insulin (26), in the liver of WT and *Atf4*$^{-/-}$ mice in basal and insulin-stimulated conditions after overnight fasting. As shown in Figure 1J and Supplemental Figure 1, A and B (supplemental material available online with this article; doi:10.1172/JCI39366DS1), phosphorylation of Akt and GSK-3β was increased in basal condition in *Atf4*$^{-/-}$ livers, and this phosphorylation was further enhanced following stimulation by insulin.

The increase in insulin sensitivity was not limited to the liver; indeed, expression of medium-chain acyl-CoA dehydrogenase (*Mcad*), a maker of insulin sensitivity in muscle, was also significantly increased in *Atf4*$^{-/-}$ mice (Figure 1K) (27). Moreover, and as shown in Figure 1L, phosphorylation of Akt was increased in basal conditions in *Atf4*$^{-/-}$ muscle, and this phosphorylation was further enhanced following stimulation by insulin. In addition, expression of *Pparg*, a marker of insulin sensitivity in fat cells, was increased in *Atf4*$^{-/-}$ mice (Figure 1K) (28). Taken together, these results indicate that *Atf4* deletion in all cells in vivo results not only in an increase in insulin secretion but also enhances insulin sensitivity in the liver, muscle, and fat cells.

Atf4 inactivation does not affect insulin sensitivity in isolated hepatocytes. We next used liver and hepatocytes to determine whether ATF4 regulates insulin sensitivity in a cell-autonomous manner, i.e., through its expression in hepatocytes. To that end, we compared expression of insulin target genes and insulin sensitivity marker genes that were analyzed in *Atf4*$^{-/-}$ livers to their expression in primary culture of hepatocytes prepared from WT and *Atf4*$^{-/-}$ mice.

To our surprise, and as shown in Figure 1I and in Supplemental Figure 1C, there was no significant difference in the expression of any of these genes between WT and *Atf4*$^{-/-}$ hepatocytes. To further confirm that insulin could signal in hepatocytes regardless of the presence or absence of ATF4 in this cell type, we studied phosphorylation of Akt and GSK-3β in WT and *Atf4*$^{-/-}$ hepatocytes. As shown in Figure 1J, Akt phosphorylation in *Atf4*$^{-/-}$ hepatocytes was similar to that of WT hepatocytes in basal conditions, and insulin enhanced this phosphorylation to a similar extent in WT and *Atf4*$^{-/-}$ hepatocytes. The level of phosphorylation of GSK-3β in *Atf4*$^{-/-}$ hepatocytes was also similar to that of WT hepatocytes in both basal and insulin-stimulated conditions (Supplemental Figure 1B). Although we cannot rule out the possibility that the absence of effect of the *Atf4* deletion in hepatocytes may be due to dedifferentiation of these cells in culture, these results suggest that insulin can signal normally in hepatocytes regardless of the presence or absence of ATF4 in this cell type. This raises the testable hypothesis that ATF4 affects insulin sensitivity, at least in liver, through its expression in another cell type.

Atf4 overexpression in osteoblasts hampers insulin secretion and insulin sensitivity. How could ATF4 inhibit insulin sensitivity in the liver in a non–cell-autonomous manner? That ATF4 accumulates mostly in osteoblasts (5) along with the metabolic functions recently ascribed to this cell type (10) suggested that it may be, at least in part, through its osteoblastic expression that *Atf4* affects glucose metabolism.

As an initial means to addressing this question, we relied on the use of transgenic mice overexpressing *Atf4*. Specifically, we compared mice overexpressing *Atf4* in osteoblasts but in no other tissues [α1(I)Collagen-Atf4 mice] to transgenic mice overexpressing *Atf4* in all tissues but not in bone (*CMV-Atf4* mice). We verified, prior to analyzing these mice, that the α1(I)Collagen-Atf4 transgene was not expressed in pancreas, white adipose tissue, liver, muscle, and brain, while the *CMV-Atf4* transgene was expressed in all tissues examined but had a markedly weaker expression in bone compared with other tissues (Figure 2A and Supplemental Figure 2). The specificity of expression of ATF4 was further verified at the protein level (Supplemental Figure 2, A and B). We also determined that in the bones of α1(I)Collagen-Atf4 mice, *Atf4* expression was 60% higher than in WT bones (Figure 2B).

α1(I)Collagen-Atf4 but not *CMV-Atf4* mice displayed a significant increase in blood glucose levels and a significant decrease in circulating insulin levels compared with WT littermates. Hence, α1(I)Collagen-Atf4 mice had, in first approximation, metabolic abnormalities that were opposite to what was observed in *Atf4*$^{-/-}$ mice (Figure 2, C and D).

To assess whether this decrease in circulating insulin levels betrayed a decrease in insulin secretion in the α1(I)Collagen-Atf4 mice, we performed GSIS tests, which revealed that insulin

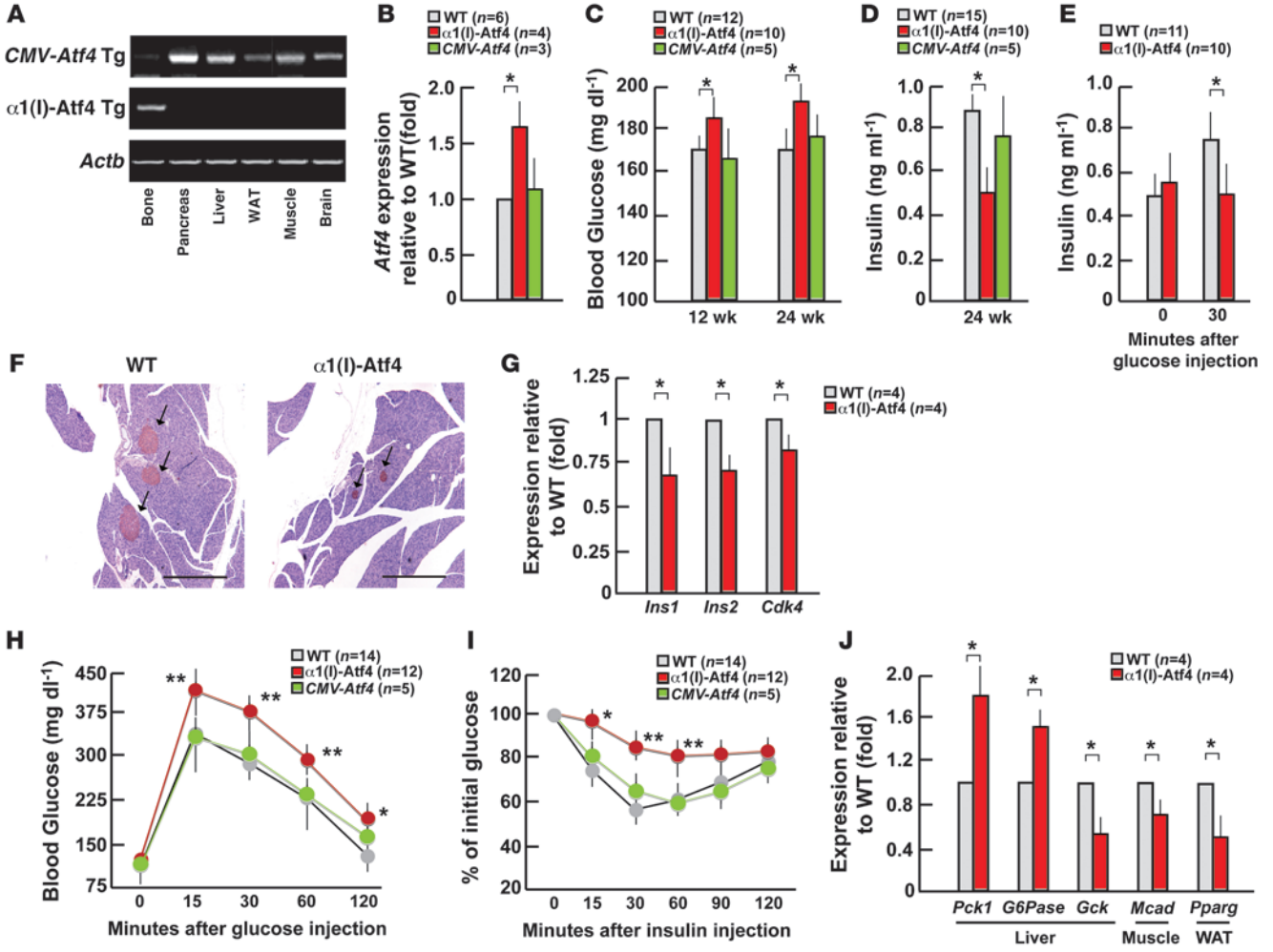

Figure 2

Overexpression of *Atf4* in osteoblasts only decreases glucose tolerance. (**A**) *CMV-Atf4* and α1(I)Collagen-Atf4 (α1(I)-Atf4) transgene expression in several tissues. (**B**) Endogenous *Atf4* expression in bone of *CMV-Atf4* and α1(I)Collagen-Atf4 mice. (**C** and **D**) Blood glucose and serum insulin levels in *CMV-Atf4* and α1(I)Collagen-Atf4 mice at indicated ages. (**E**) GSIS test in α1(I)Collagen-Atf4 mice. (**F**) Insulin immunostaining in pancreas of α1(I)Collagen-Atf4 mice. Arrows indicate islets. Scale bars: 500 μm. (**G**) *Insulin* and *Cdk4* expression in pancreas of α1(I)Collagen-Atf4 mice. (**H** and **I**) GTT and ITT in *CMV-Atf4* and α1(I)Collagen-Atf4 mice. (**J**) Insulin target genes and insulin sensitivity marker genes expression in liver, muscle and white adipose tissue in α1(I)Collagen-Atf4 mice. Analysis of 24 week-old *CMV-Atf4* and α1(I)Collagen-Atf4 mice is shown in **E**–**J**. Error bars show mean + SEM. $^{**}P < 0.01$; $^{*}P < 0.05$, WT versus α1(I)Collagen-Atf4 mice.

secretion following a glucose challenge was significantly lower in α1(I)Collagen-Atf4 mice than in WT littermates (Figure 2E). Consistent with the decrease in serum insulin levels, there was also in α1(I)Collagen-Atf4 mice a significant decrease in islet insulin content, in insulin immunoreactivity, in β cell area and mass, and in *Ins* expression (Figure 2, F and G, and Table 2). In addition, the number of Ki67-positive β cells and the expression of *Cdk4*, a regulator of cell cycle affecting β cell proliferation (29), were also significantly decreased in pancreas of α1(I)Collagen-Atf4 mice (Figure 2G and Table 2).

To determine how this decrease in insulin secretion could affect the ability of α1(I)Collagen-Atf4 mice to dispose of a glucose load, we performed a GTT. This test showed that α1(I)Collagen-Atf4 mice had a significantly lower tolerance to glucose than WT mice (Figure 2H). We next asked whether the glucose intolerance of the α1(I)Collagen-Atf4 mice was caused in part by a decrease in insulin sensitivity. An ITT showed that insulin sensitivity was significantly decreased in α1(I)Collagen-Atf4 mice compared with WT mice (Figure 2I), although the circulating levels of adipokines affecting this process, such as leptin, resistin, and adiponectin, were not affected in α1(I)Collagen-Atf4 mice (Supplemental Figure 3). In addition, α1(I)Collagen-Atf4 mice showed increased expression of *Pck1* and *G6pase* and decreased *Gck* expression in the liver and decreased expression of *Pparg* in fat cells and *Mcad* in muscle (Figure 2J). Consistent with the virtual absence of the *CMV-Atf4* transgene in bone, none of these metabolic and histological abnormalities were observed in *CMV-Atf4* mice (Figure 2, B–D, H, and I, and Table 2). Thus, *Atf4* overexpression in osteoblasts only results in a metabolic phenotype that is the mirror image of the one observed in *Atf4*$^{-/-}$ mice, while its overexpression in other tissues does not.

We next introduced the α1(I)Collagen-Atf4 transgene in *Atf4*$^{-/-}$ mice [α1(I)Collagen-Atf4;*Atf4*$^{-/-}$ mice], reasoning that the extent of

Table 2
Insulin contents, β cell area, β cell mass, and quantification of insulin/Ki67-positive cells in *CMV-Atf4* and α1(I)Collagen-Atf4 mice

	WT ($n \geq 6$)	α1(I)Collagen-Atf4 ($n \geq 6$)	*CMV-Atf4* ($n \geq 4$)
Insulin content (ng/mg pancreas)	134.1 ± 10.9	97.1 ± 12.6[A]	ND
β cell area (%)	1.07 ± 0.30	0.58 ± 0.18[A]	0.95 ± 0.20
β cell mass (mg)	3.87 ± 0.18	1.95 ± 0.21[A]	3.45 ± 0.37
Ki67-positive cells (%)	1.42 ± 0.21	0.81 ± 0.32[A]	ND

[A]$P < 0.05$, WT versus α1(I)Collagen-Atf4 mice. Analysis is of 24-week-old mice. ND, not determined.

the rescue of the metabolic phenotype of the *Atf4*$^{-/-}$ mice induced by this transgene would be a reliable, albeit suggestive, indicator of the role that *Atf4* expression in osteoblasts plays in regulating glucose metabolism. Remarkably, *Atf4* expression was restored to a WT level but not above it in the bones of α1(I)Collagen-Atf4;*Atf4*$^{-/-}$ mice (Figure 3A). As shown in Figure 3, B–L, whether we looked at blood glucose, circulating insulin levels, metabolic tests (GTT, ITT, GSIS test, and PTT), pancreas histology, or gene expression in islets, liver, and muscle, the α1(I)Collagen-Atf4 transgene completely rescued the metabolic abnormalities of the *Atf4*$^{-/-}$ mice.

Inactivation of Atf4 only in osteoblasts increases insulin secretion and enhances insulin sensitivity. The data presented above all pointed toward the intriguing possibility that ATF4 might regulate insulin secretion and insulin sensitivity through its expression in osteoblasts. To determine more definitely that this was indeed the case, we generated mice lacking *Atf4* only in osteoblasts by crossing *α1(I)collagen-Cre* mice (30) with mice harboring a floxed allele of *Atf4* (Supplemental Figure 4). These *α1(I)Collagen-Cre;Atf4*$^{fl/fl}$ (*Atf4*$_{osb}^{-/-}$) mice were subjected to the same tests as *Atf4*$^{-/-}$ and α1(I)Collagen-Atf4 mice. As a negative control, we used mice lacking, in osteoblasts only, another member of the same family of transcription factors, CREB [*α1(I)Collagen-Cre;Creb*$^{fl/fl}$ (*Creb*$_{osb}^{-/-}$) mice].

Starting at 2 weeks of age, we noticed the same significant decrease in blood glucose levels in *Atf4*$_{osb}^{-/-}$ mice that we had observed in mice lacking *Atf4* in all cells. These markedly lower blood glucose levels were also observed at 1 month of age in *Atf4*$_{osb}^{-/-}$ mice (Figure 4A). In addition, *Atf4*$_{osb}^{-/-}$ but not *Creb*$_{osb}^{-/-}$ mice showed a significant increase in circulating insulin levels and in insulin secretion following a glucose challenge (GSIS test) compared with control littermates (Figure 4, B and C). To determine whether *Atf4*$_{osb}^{-/-}$ mice were more tolerant to a glucose load than control littermates, we performed GTT after overnight fasting. The GTT showed that *Atf4*$_{osb}^{-/-}$ mice, like *Atf4*$^{-/-}$ mice, were significantly more tolerant to a glucose challenge than control littermates (Figure 4D; compare with Figure 1F).

To assess insulin sensitivity in the *Atf4*$_{osb}^{-/-}$ mice, we first performed an ITT, which showed that insulin sensitivity was increased in *Atf4*$_{osb}^{-/-}$ mice to the same extent as in *Atf4*$^{-/-}$ mice when compared with control littermates (Figure 4E; compare with Figure 1G). Again, this increase in insulin sensitivity occurred in the face of normal levels of circulating adipokines (Supplemental Figure 3). We next performed PTT in *Atf4*$_{osb}^{-/-}$ mice. There was also, in *Atf4*$_{osb}^{-/-}$ mice, a reduction in glucose production after pyruvate challenge similar to the one seen in *Atf4*$^{-/-}$ mice (Figure 4F; compare with Figure 1H). That the expression of *Pck1* and *G6pase* was reduced in the liver of *Atf4*$_{osb}^{-/-}$ mice further confirmed that gluconeogenesis was reduced in these mutant mice (Figure 4G). Moreover, there was also, as we had observed in *Atf4*$^{-/-}$ mice, a significant increase in the expression of *Gck* in the liver, *Mcad* in the muscle, and *Pparg* in the fat cells of *Atf4*$_{osb}^{-/-}$ mice (Figure 4G). None of these abnormalities were observed in *Creb*$_{osb}^{-/-}$ mice (Figure 4, A, B, D, and E, and Supplemental Figure 3). Last, to further assess insulin sensitivity, we performed a 2-hour hyperinsulinemic-euglycemic clamp in conscious mice (Supplemental Table 1). *Atf4*$_{osb}^{-/-}$ mice had lower basal glucose levels than WT littermates (95 ± 9 vs. 120 ± 13 mg/dl in WT mice). During the clamp, plasma glucose levels were maintained at euglycemia (~110 mg/dl) in both groups of mice. Steady-state rates of glucose infusion to maintain euglycemia during the clamp were significantly elevated in *Atf4*$_{osb}^{-/-}$ mice compared with the WT mice (69 ± 3 vs. 47 ± 4 mg/kg/min in WT mice; $P = 0.01$). This was mostly due to a 40% increase in insulin-stimulated whole-body glucose turnover in *Atf4*$_{osb}^{-/-}$ mice (70 ± 3 vs. 50 ± 4 mg/kg/min in WT mice; $P = 0.02$). Insulin-stimulated whole-body glycogen synthesis was markedly elevated in *Atf4*$_{osb}^{-/-}$ mice (42 ± 4 vs. 17 ± 7 mg/kg/min in WT mice; $P = 0.04$). Taken together, these data are consistent with the notion that ATF4 decreases insulin secretion and hampers insulin sensitivity through its expression in osteoblasts.

ATF4 directly regulates Esp expression in osteoblasts. Since ATF4 is a known regulator of the expression of osteocalcin, a gene favoring insulin secretion and insulin sensitivity (4, 10), the observation that *Atf4*$^{-/-}$ mice had a glucose metabolism phenotype mirroring the one seen in *Osteocalcin*$^{-/-}$ mice was counterintuitive and raised the hypothesis that ATF4 could regulate expression in osteoblasts of a gene or genes that oppose the metabolic function of osteocalcin. One such gene is *Esp*, which acts upstream of osteocalcin (10). Remarkably, the metabolic phenotypes of *Esp*$^{-/-}$, *Atf4*$^{-/-}$, and *Atf4*$_{osb}^{-/-}$ mice are strikingly similar.

Analysis of the *Esp* promoter revealed the existence of a cAMP-responsive element (CRE) at –340. To assess the importance of this cis-acting element in regulating *Esp* expression in osteoblasts, we performed DNA transfection assays in ROS17/2.8 cells, an osteoblastic cell line expressing *Esp* (10). A construct containing a 600-bp *Esp* promoter fragment cloned upstream of a luciferase (*luc*) gene (*pEsp600-luc*) was more than 10 times more active than a construct containing a shorter *Esp* promoter that did not include this CRE element (*pEsp300-luc*) (Figure 5A). We interpreted these experiments as suggesting that sequences between –600 and –300 of the *Esp* promoter, including the CRE, were necessary for its osteoblast-specific activity in cell culture (Figure 5A).

Next, we performed DNA cotransfection experiments in COS cells that do not express *Esp*. Cotransfection of a *Runx2* or of a *Creb* expression vector did not have an effect on the activity of *pEsp-luc*, while an expression vector for *Atf4* consistently increased its activity (Figure 5B). We also used in DNA cotransfection experiments an artificial promoter containing 6 copies of the CRE located at –340 in the *Esp* promoter cloned upstream of luc (*p6Esp-luc*). The *Atf4* expression vector increased the activity of *p6Esp-luc* 8-fold but did not transactivate a construct containing a mutation in this site (*p6Esp(m)-luc*) that prevents binding of nuclear proteins to this sequence (Figure 5C). Unlike ATF4, CREB did not transactivate *p6Esp-luc*, although it could transactivate a reporter construct containing a consensus CREB-binding site used here as a positive control (*pCreb-luc*) (Figure 5C).

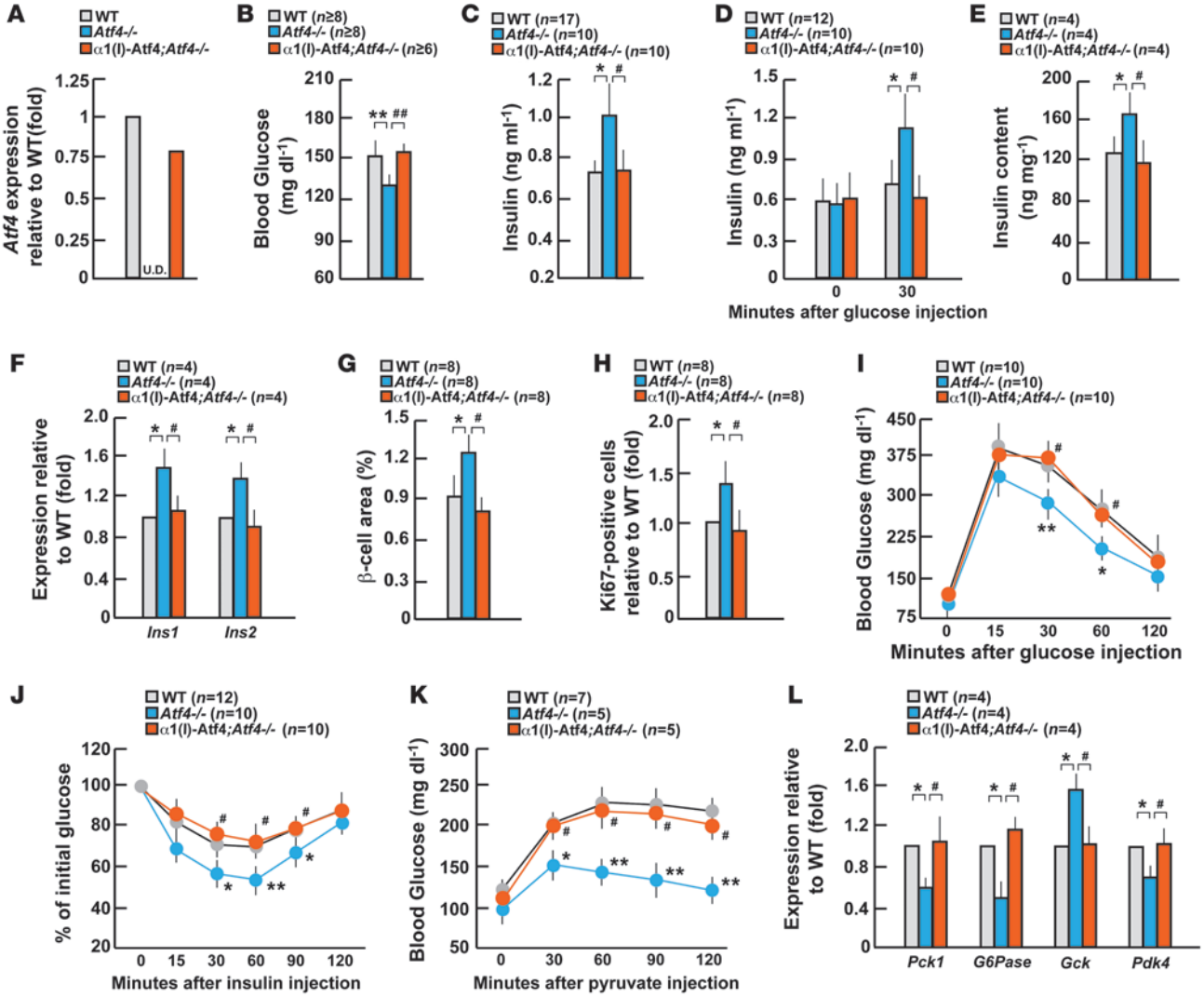

Figure 3

Atf4 introduction in osteoblasts rescues glucose tolerance in *Atf4*$^{-/-}$ mice. (**A**) Endogenous *Atf4* expression in bone of α1(I)Collagen-Atf4;*Atf4*$^{-/-}$ mice. (**B** and **C**) Blood glucose and serum insulin levels in α1(I)Collagen-Atf4;*Atf4*$^{-/-}$ mice. (**D**) GSIS test in α1(I)Collagen-Atf4;*Atf4*$^{-/-}$ mice. (**E**–**H**) Insulin contents, *Insulin* expression in pancreas, β cell area, and quantification of insulin/Ki67-positive cells in α1(I)Collagen-Atf4;*Atf4*$^{-/-}$ mice. (**I**–**K**) GTT, ITT, and PTT in α1(I)Collagen-Atf4;*Atf4*$^{-/-}$ mice. (**L**) Insulin target gene expression in the liver of α1(I)Collagen-Atf4;*Atf4*$^{-/-}$ mice. Analysis of 8-week-old α1(I)Collagen-Atf4;*Atf4*$^{-/-}$ mice is shown in **A**–**L**. Error bars show mean + SEM. $^{**}P < 0.01$; $^{*}P < 0.05$, WT versus *Atf4*$^{-/-}$ mice; $^{\#\#}P < 0.01$; $^{\#}P < 0.05$, *Atf4*$^{-/-}$ versus α1(I)Collagen-Atf4;*Atf4*$^{-/-}$ mice. U.D., underdetected.

ChIP assays confirmed that ATF4 but not CREB binds to the CRE element in the *Esp* promoter (Figure 5D). The specificity of the binding of ATF4 to the CRE element located at –340 in the *Esp* promoter was verified by electric mobility shift assay. In that assay, we used as a source of proteins nuclear extracts of 293 cells transfected with either an empty vector or a vector expressing a FLAG-tagged version of ATF4. As shown in Figure 5E, a protein-DNA complex formed upon incubation of a labeled double-stranded oligonucleotide encompassing the sequence of the –340 CRE elements with nuclear extracts of 293 cells transfected with the ATF4 expression vector (Figure 5E) but not when nuclear extracts of cells transfected with the empty vector were used (data not shown). As a control of specificity we also performed "supershift" experiments using various antibodies. As shown in Figure 5E, an antibody against the FLAG sequence could alter the mobility of the protein-DNA complex, while an antibody against an unrelated sequence could not (Figure 5E).

Taken together, these data indicate that the CRE element present at –340 bp in the *Esp* promoter is required, at least in cell culture, for the osteoblast-specific activity of the *Esp* promoter. These molecular observations are consistent with the existence of a metabolic phenotype in *Atf4*$_{osb}^{-/-}$ mice but not in *Creb*$_{osb}^{-/-}$ mice and with the fact that *Esp* expression was significantly increased in α1(I)Collagen-Atf4 mice and decreased in *Atf4*$_{osb}^{-/-}$ mice but not affected in *Creb*$_{osb}^{-/-}$ mice (Figure 5F).

ATF4 modulates glucose metabolism via osteocalcin by favoring Esp expression in osteoblasts. To further ascertain that it is through its regulation of *Esp* expression that ATF4 achieves its function on metabolism, we performed 3 additional experiments.

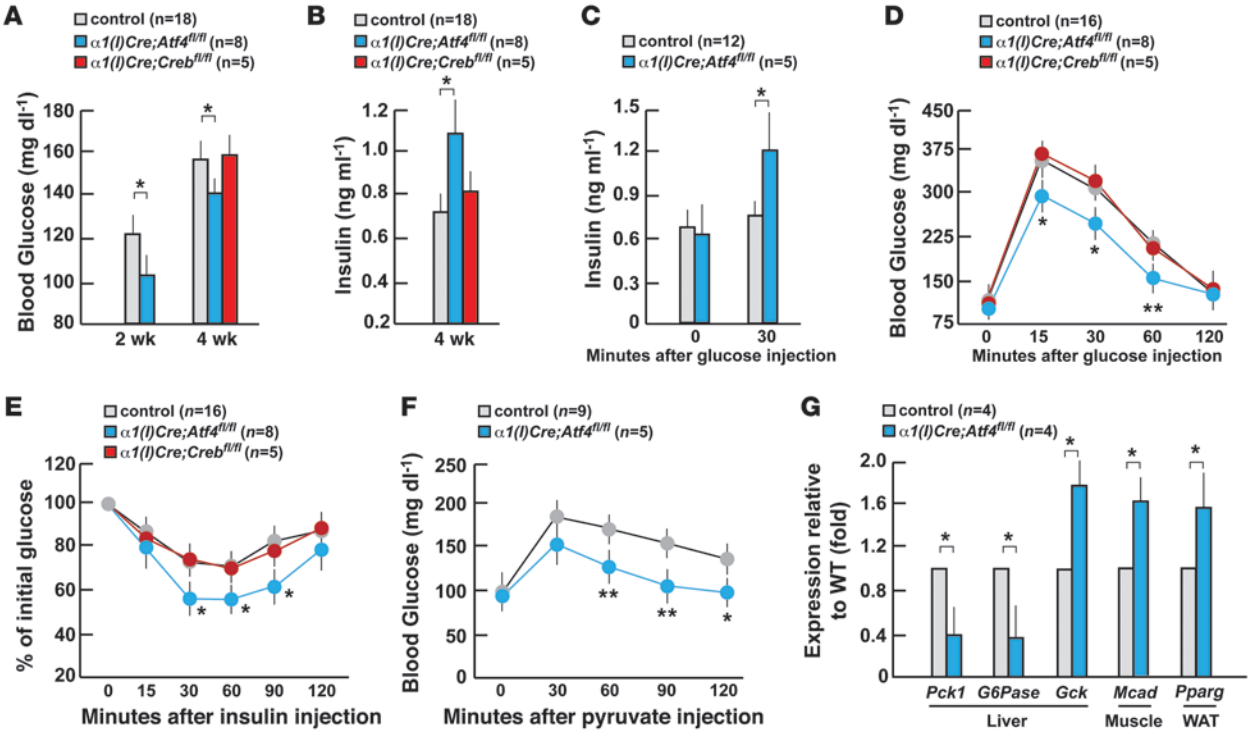

Figure 4

Inactivation of *Atf4* only in osteoblasts increases glucose tolerance. (**A** and **B**) Blood glucose and serum insulin levels in $Atf4^{fl/fl}$ [$\alpha 1(I)Collagen\text{-}Cre;Atf4^{fl/fl}$ ($\alpha 1(I)Cre;Atf4^{fl/fl}$)], and $Creb_{osb}^{-/-}$ [$\alpha 1(I)Collagen\text{-}Cre;Creb^{fl/fl}$ ($\alpha 1(I)Cre;Creb^{fl/fl}$)] mice at indicated ages. (**C**) GSIS test in $Atf4_{osb}^{-/-}$ mice. (**D** and **E**) GTT and ITT in $Atf4_{osb}^{-/-}$ and $Creb_{osb}^{-/-}$ mice. (**F**) PTT in $Atf4_{osb}^{-/-}$ mice. (**G**) Insulin target gene and insulin sensitivity marker gene expression in liver, muscle, and white adipose tissue of $Atf4_{osb}^{-/-}$ mice. Analysis of 4-week-old $Atf4_{osb}^{-/-}$ and $Creb_{osb}^{-/-}$ mice is shown in **C**–**G**. Error bars show mean + SEM. $^{**}P < 0.01$; $^{*}P < 0.05$, WT versus $Atf4_{osb}^{-/-}$ mice.

First, we generated compound heterozygous mice lacking 1 allele of *Atf4* and 1 allele of *Esp*. As shown in Figure 6, A–C, while $Atf4^{+/-}$ mice and $Esp^{+/-}$ mice were indistinguishable from WT mice, $Atf4^{+/-}Esp^{+/-}$ mice displayed a metabolic phenotype similar to that of the $Esp^{-/-}$ mice whether we looked at blood glucose levels, serum insulin levels, or the number of Ki67/Insulin-positive β cells, and *Esp* expression was significantly decreased in the compound heterozygous mice (data not shown). Furthermore, the percentage of uncarboxylated osteocalcin was significantly increased in $Atf4^{+/-}Esp^{+/-}$ compared with control mice (Supplemental Figure 6). These data indicate that *Atf4* and *Esp* are in the same genetic pathway. Second, since *Esp* favors osteocalcin carboxylation, a posttranslational modification that hampers osteocalcin metabolic function (10), we measured osteocalcin carboxylation in WT, α1(I)Collagen-Atf4, and $Atf4_{osb}^{-/-}$ mice. As shown in Figure 6D, the percentage of uncarboxylated osteocalcin, i.e., bioactive osteocalcin, present in serum was decreased in α1(I)Collagen-Atf4 mice compared with WT. In contrast, this percentage was increased in $Atf4_{osb}^{-/-}$ mice to the same extent as in $Esp^{-/-}$ mice, although the level of serum total osteocalcin was decreased in $Atf4_{osb}^{-/-}$ mice (Supplemental Figure 5).

If uncarboxylated osteocalcin is a mediator of the metabolic functions of ATF4 present in osteoblasts, then one would expect that adding exogenous uncarboxylated osteocalcin to α1(I)Collagen-Atf4 mice would rescue their metabolic phenotypes. Indeed, and as shown in Figure 6, E–G, the metabolic abnormalities noticed in the α1(I)Collagen-Atf4 mice were rescued by long-term perfusion of uncarboxylated osteocalcin. Taken together, these data indicate that ATF4 regulates glucose metabolism, at least in part, by favoring expression of *Esp* in osteoblasts and, as a result, by decreasing osteocalcin bioactivity. That a single injection of warfarin (77 μg/kg), a compound that inhibits the carboxylation of osteocalcin (31), decreased blood glucose levels in WT mice and did so even more severely in α1(I)Collagen-Atf4 mice, but not in $Osteocalcin^{-/-}$ mice (Figure 6H), added further credence to this contention.

Discussion

In this report, we provide in vivo evidence indicating that the transcription factor ATF4 negatively regulated insulin secretion and decreases sensitivity to insulin in liver, muscle, and fat cells; we show that it achieves this function, in large part, through its expression in osteoblasts. Last, we provide a molecular explanation for this set of observations (see Figure 7).

ATF4 has already been implicated in many critically important cellular processes. For instance, its translation increases in the case of amino acid starvation and ER stress following phosphorylation of eIF2α. ATF4 then initiates a gene expression program promoting amino acid import into cells (6). Although *Atf4* is a broadly expressed gene (4), the main phenotypic abnormalities noted in $Atf4^{-/-}$ mice after birth are in the skeleton. This is due, to a large extent, to the fact that the ATF4 protein is far more abundant in osteoblasts than in any other cell type analyzed (5). This restricted accumulation in osteoblasts explains why ATF4 is such an impor-

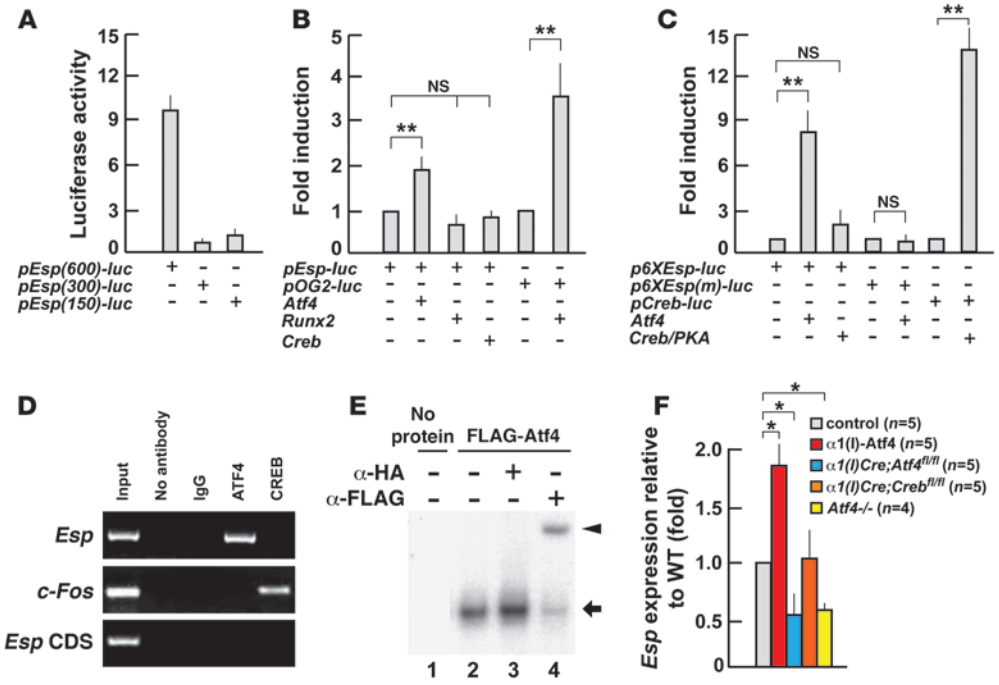

Figure 5

ATF4 directly regulates Esp expression in osteoblasts. (**A**) DNA transfection assay in ROS17/2.8 osteoblasts with different length of *Esp* promoters. (**B**) DNA cotransfection assay in COS cells using *Esp* promoter and indicated expression vectors. (**C**) DNA cotransfection assay in COS cells using *Esp* promoter containing 6 copies of the CRE site or mutated CRE site and indicated expression vectors. (**D**) ChIP assay in primary calvarial osteoblasts using ATF4 and CREB antibodies. (**E**) Electric mobility shift assay using labeled CRE site located at –340 in the *Esp* promoter and FLAG-Atf4 protein. (**F**) *Esp* expression in bone of 8-week-old α1(I)Collagen-Atf4, $Atf4_{osb}^{-/-}$, $Creb_{osb}^{-/-}$, *and* $Atf4^{-/-}$ mice. $^{**}P < 0.01$; $^{*}P < 0.05$, WT versus α1(I)Collagen-Atf4 or $Atf4_{osb}^{-/-}$ mice (**E**).

tant determinant of collagen synthesis, bone formation, and through its regulation of *Rankl*, osteoclast differentiation (4, 9). The paramount importance of ATF4 in bone biology before and even more after birth is also illustrated by the fact that its activity is affected in several human diseases and mouse models of these conditions. For instance, ATF4 transcriptional activity is decreased and bone formation is hampered in a mouse model of Coffin-Lowry syndrome (4), a rare skeletal dysplasia, while it is increased, as is bone formation, in a mouse model recapitulating some of the skeletal manifestation of neurofibromatosis type I (7).

That ATF4 regulates such a large number of functions fulfilled by osteoblasts suggested that this transcription factor may also affect other aspects of osteoblast biology such as, for instance, the recently described ability of this cell type to improve glucose metabolism (10). In indirect support of this hypothesis, one other disease, Wolcott-Rallison syndrome (WRS), affecting among other organs the skeleton, is caused by inactivating mutations in the gene encoding *EIF2AK3* (13). This mutation should prevent any increased translation of *Atf4* following ER stress or amino acid starvation, although it may change many other functions. WRS patients are also diabetic, suggesting that ATF4 could be needed for insulin secretion (13).

Results of the present analysis demonstrate that, unlike what could have been anticipated, ATF4 inhibits insulin secretion as well as insulin sensitivity. Furthermore, cell-specific gain-of-function and loss-of-function experiments in mice establish that it is, to a large extent, through its osteoblastic expression that ATF4 regulates these 2 functions. In this cell type, ATF4 regulates the expression of *Esp*, a gene inhibiting the metabolic functions of osteocalcin, a bone-derived secreted molecule promoting insulin secretion and insulin sensitivity (10). Thus, although ATF4 regulates the expression of both *Osteocalcin* and *Esp*, it is through the regulation of the latter gene that ATF4 inhibits insulin secretion and insulin sensitivity. Indeed, by increasing *Esp* expression, ATF4 decreases the ability of osteocalcin to increase insulin secretion (12). This function of the osteoblast-expressed *Atf4* is consistent with the fact that ATF4 function is regulated by the sympathetic tone, which also regulates *Esp* expression, and by protein intake (7, 9, 12).

We remain aware, however, that our results do not exclude the formal possibility that ATF4 may also exert an influence on glucose metabolism in addition to the mechanism of action presented here through its expression in other cell types such as the adipocyte. This note of caution is an important one since, for instance, the levels of adiponectin are not affected in $Atf4^{-/-}$ or in α1(I)Collagen-Atf4–overexpressing mice. This may be an indication that ATF4, through its expression in osteoblasts, modulates glucose metabolism via an osteocalcin-independent mechanism. Alternatively, we cannot exclude the possibility that osteocalcin regulates insulin sensitivity in adipocytes, hepatocytes, and myoblasts directly, without any intervention of adiponectin. That *Atf4* and *Esp* lie in the same genetic cascade provides some support to the latter hypothesis. These are the 2 important issues that will need to be addressed once a specific receptor for osteocalcin has been molecularly identified.

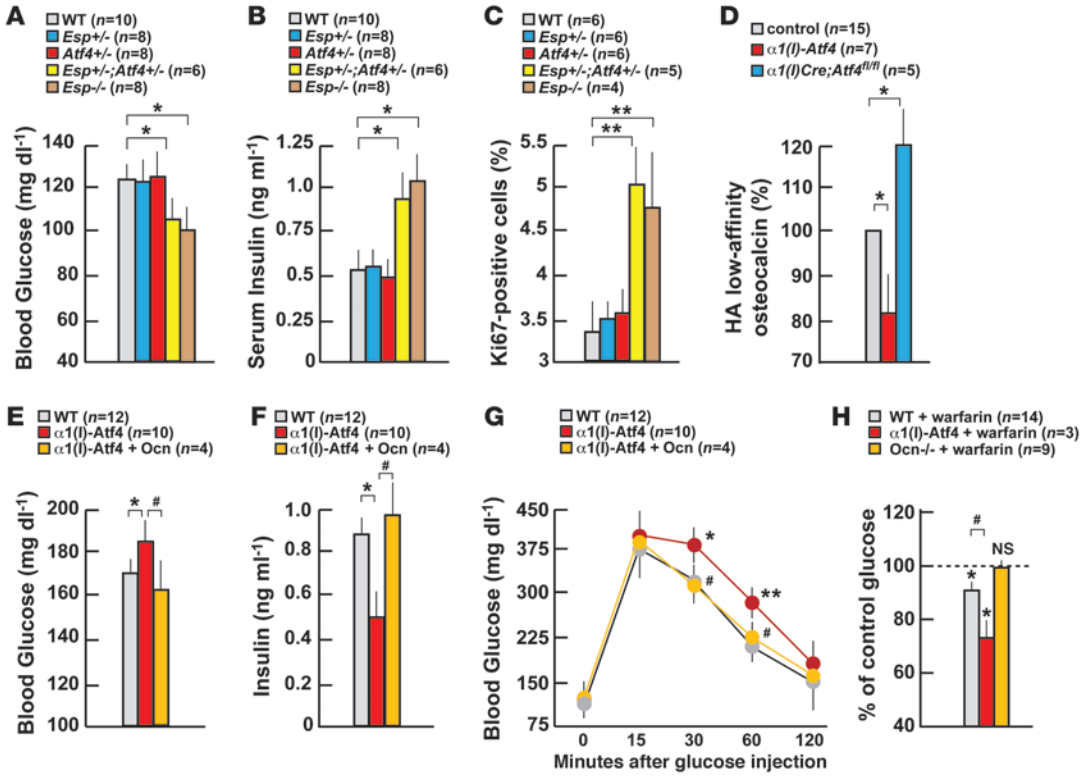

Figure 6

ATF4 modulates glucose metabolism through regulation of osteocalcin bioactivity by favoring *Esp* expression in osteoblasts. (**A**–**C**) Blood glucose, serum insulin levels, and quantification of insulin/Ki67-immunoreactive cells in islets of 2-week-old $Esp^{+/-}Atf4^{+/-}$ mice. (**D**) Serum uncarboxylated osteocalcin levels in α1(I)Collagen-Atf4 and $Atf4_{osb}^{-/-}$ mice. (**E** and **F**) Blood glucose and serum insulin levels in uncarboxylated osteocalcin-treated α1(I)Collagen-Atf4 mice. (**G**) GTT in uncarboxylated osteocalcin-treated α1(I)Collagen-Atf4 mice. (**H**) Blood glucose (percentage of DMSO-treated control) at 60 minutes after injection in warfarin-treated α1(I)Collagen-Atf4 mice and $Ocn^{-/-}$ mice. Analysis shows 12-week-old α1(I)Collagen-Atf4 mice in **E**–**G**. Analysis shows 24-week-old α1(I)Collagen-Atf4 mice and $Ocn^{-/-}$ mice in **H**. Error bars show mean + SEM. $^{**}P < 0.01$; $^{*}P < 0.05$, WT versus $Esp^{+/-}Atf4^{+/-}$ or $Esp^{-/-}$ mice (**A**–**C**), WT versus α1(I)Collagen-Atf4 or $Atf4_{osb}^{-/-}$ mice (**D**) WT versus α1(I)Collagen-Atf4 mice (**E**–**G**), DMSO-treated mice as control versus warfarin-treated mice (**H**). $^{\#}P < 0.05$, α1(I)Collagen-Atf4 versus osteocalcin-treated α1(I)Collagen-Atf4 mice (**E**–**G**), WT mice plus warfarin versus α1(I)Collagen-Atf4 mice plus warfarin (**H**).

As mentioned above, ATF4 was already known to regulate bone formation and mineralization as well as osteoclast differentiation through its osteoblast expression (7–9). By showing that it is also involved in the endocrine function of this cell, this study underscores the critical importance of ATF4 as a regulator of many, but not all, the functions of this cell type. To date, the only function of the osteoblast that is not influenced by ATF4 is the regulation of phosphate metabolism (data not shown). By identifying another regulatory gene involved in this pathway, the observations presented in the paper add further credence to the notion that the osteoblast is a bona fide endocrine cell.

Methods

Animals. α1(I)Collagen-Atf4, $Esp^{-/-}$, *Creb-flox/flox*, $Atf4^{-/-}$, and *α1(I)Collagen-Cre* mice were previously described (4, 7, 30, 32, 33). *Creb-flox/flox* mice were a gift from G. Schütz (German Cancer Research Center, Heidelberg, Germany). Osteoblast-specific *Atf4*-deficient mice ($Atf4_{osb}^{-/-}$) mice were generated through homologous recombination in ES cells and the use

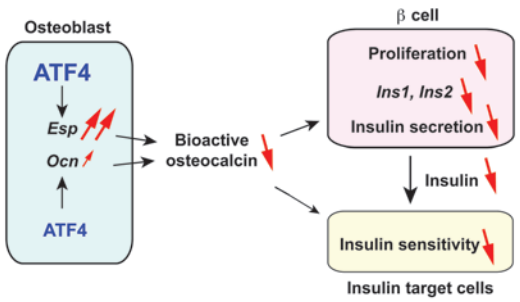

Figure 7

Model showing how ATF4 controls glucose handling through its expression in osteoblasts. ATF4 controls the expression of *Osteocalcin* (*Ocn*) and to a larger extent of *Esp*, a gene encoding an inhibitor of osteocalcin bioactivity. This causes a chronic decrease in osteocalcin-mediated insulin production and induces a long-term negative effect on pancreatic β cell proliferation. At the same time, the sensitivity to insulin of its target tissues (liver, fat, and muscle) is decreased.

of α*1(I)Collagen-Cre* transgenic mice (30). Genotyping was performed by PCR analysis of genomic DNA. All mutant mouse strains were on the same genetic background (C57BL6/J) except for the α1(I)Collagen-Atf4 transgenic mice, which were generated on an Fvb background. All procedures involving animals were approved by the Columbia University IACUC. The Columbia University IACUC meets national standards.

Metabolic studies. For GTT, glucose (2 g/kg) was injected i.p. after overnight fast, and blood glucose was monitored using blood glucose strips and the Accu-Check glucometer (Roche) at indicated times. For PTT, pyruvate (2 g/kg) was injected i.p. after overnight fast, and blood glucose levels were measured at indicated times. For ITT, insulin (0.5 or 0.75 U/kg) was injected i.p. after 4 hours of fasting, and blood glucose levels were measured at indicated times. ITT data are presented as percentage of initial blood glucose concentration. For GSIS test, glucose was injected (3 g/kg) i.p. after overnight fast. Serum was then collected from tail veins at the indicated times. Serum insulin levels were subsequently measured by ELISA (Mercodia). Hyperinsulinemic-euglycemic clamps were performed as previously described (10). In brief, $Atf4_{osb}^{-/-}$ and control littermates ($n = 3$ for each group) were fasted overnight, and 2-hour hyperinsulinemic-euglycemic clamps were performed following i.v. administration of [3-3H] glucose and 2-deoxy-D-[1-14C] glucose. Warfarin (77 μg/kg) or DMSO diluted in saline solution was injected in mice, and blood glucose was measured 60 minutes later.

Insulin signaling studies. Primary hepatocytes were isolated from adult mice as previously described (34). In brief, the liver was perfused by cannulation in the portal vein with HBSS containing 0.125 mM EGTA, followed by perfusion with HBSS containing 0.3 mM $CaCl_2$, 100 U/ml collagenase, (Wako), and 120 μg/ml trypsin inhibitor (Sigma-Aldrich). The liver then was removed and filtered through a cell strainer at 100 μm followed by washing with William's E medium. The cells were plated on a type I collagen–coated dish in William's E medium containing 10% FBS. For insulin signaling study in vitro, hepatocytes were cultured in William's E medium without FBS for 24 hours and subsequently treated with insulin at 2 nM for 5 minutes, followed by homogenization with lysis buffer containing 25 mM Tris-HCl (pH 7.4), 1% NP40, 10 mM Na_3VO_4, 100 mM NaF, 10 mM $Na_4P_2O_7$, 10 mM EGTA, 10 mM EDTA, and protease inhibitors. For insulin signaling study in vivo, insulin (0.05 U/kg) was injected into the anesthetized mice through the inferior vena cava. After 5 minutes, the liver and soleus muscle were removed, followed by homogenization in the lysis buffer. The lysates from hepatocytes, liver, or muscle were subjected to immunoblotting using anti–phospho-Akt (Ser473), anti-Akt, anti–phospho–GSK-3β (Ser9), and anti–GSK-3β (Cell Signaling Technology).

Molecular studies. Primary osteoblasts were prepared from calvaria of 5-day-old pups as previously described (4) and were cultured in αMEM/10% FBS in the presence of 100 μg/ml ascorbic acid and 5 mM β-glycerophosphate for 5 days. Real-time PCR was performed on DNaseI-treated total RNA converted to cDNA using Taq SYBR Green Supermix with ROX (Bio-Rad) on an MX3000 instrument (Stratagene); β-actin amplification was used as an internal reference for each sample. ChIP assays were performed using primary calvarial osteoblasts as previously described (9). COS cells and ROS17/2.8 were transfected as described (4) using 0.5 μg of various luciferase reporter vectors, 0.05 μg of RSV–β-gal reporter vectors, and 0.5 μg each of expression plasmids unless otherwise indicated. Luciferase and β-gal assays were performed using standard procedures.

Biochemistry. Serum levels of insulin (Mercodia), adiponectin and resistin (Linco), and leptin (Crystal Chem) were measured using a commercial kit. For quantification of uncarboxylated levels of osteocalcin, sera were incubated with hydroxyapatite slurry (Sigma-Aldrich) for 1 hour. The amount of osteocalcin present in the unbound fraction and in the fractions eluted at 0.02 M and 1 M sodium phosphate (pH 6.8) was measured by IRMA (Immunotopics). Western blotting was performed as previously described (8). Anti-Atf4 (C-20) antibody was purchased from Santa Cruz Biotechnology Inc. Anti–phospho-Akt (Ser473), anti-Akt, anti–phospho–GSK-3β (Ser9), and anti–GSK-3β were purchased from Cell Signaling Technology.

Histology. Pancreas was fixed in 10% neutral formalin, embedded in paraffin, and sectioned at 5 μm; sections were stained with H&E. Immunohistochemistry was performed using rabbit anti-insulin (Santa Cruz Biotechnology Inc.) and mouse anti-Ki67 (Vector Laboratories) antibodies. β cell area represents the surface positive for insulin immunostaining divided by the total pancreatic surface. β cell mass was calculated as β cell area multiplied by pancreatic weight as described previously (10).

Electric mobility shift assay. Nuclear extracts of FLAG or FLAG-ATF4–transfected 293 cells were incubated with a –350-bp *Esp* region–containing oligonucleotide and then subjected to electrophoresis. The ATF4-bound complex and the position of a supershifted complex are indicated (Figure 5E).

Recombinant osteocalcin treatment in vivo. Purification of bacterially produced mouse recombinant uncarboxylated osteocalcin was performed as described previously (11). Eight-week-old mice were implanted s.c. with 28-day osmotic pumps (Alzet) filled with a solution of recombinant osteocalcin (3 ng/h).

Statistics. Results are given as mean ± SEM. Statistical analyses were performed using unpaired, 2-tailed Student's *t* test or ANOVA test. Significance was defined as $P < 0.05$.

Acknowledgments

We thank G. Schütz for *Creb-flox/flox* mice; P. Ducy for critical reading of the manuscript; and H. Liu and G. Ren for technical assistance. This work was supported by the Japan Society for the Promotion of Science, the Uehara Memorial Foundation, the Kanae Foundation for the Promotion of Medical Science (E. Hinoi), the Fond de la recherche en santé du Québec (M. Ferron), and the NIH (G. Karsenty).

Received for publication March 30, 2009, and accepted in revised form June 10, 2009.

Address correspondence to: Gerard Karsenty, 701 West 168th Street, Room 1602A HHSC, New York New York 10032, USA. Phone: (212) 305-4011; Fax: (212) 923-2090; E-mail: gk2172@columbia.edu.

1. Karsenty, G., and Wagner, E.F. 2002. Reaching a genetic and molecular understanding of skeletal development. *Dev. Cell.* **2**:389–406.
2. Ducy, P., Zhang, R., Geoffroy, V., Ridall, A.L., and Karsenty, G. 1997. Osf2/Cbfa1: a transcriptional activator of osteoblast differentiation. *Cell.* **89**:747–754.
3. Nakashima, K., et al. 2002. The novel zinc finger-containing transcription factor osterix is required for osteoblast differentiation and bone formation. *Cell.* **108**:17–29.
4. Yang, X., et al. 2004. ATF4 is a substrate of RSK2 and an essential regulator of osteoblast biology; implication for Coffin-Lowry Syndrome. *Cell.* **117**:387–398.
5. Yang, X., and Karsenty, G. 2004. ATF4, the osteoblast accumulation of which is determined post-translationally, can induce osteoblast-specific gene expression in non-osteoblastic cells. *J. Biol. Chem.* **279**:47109–47114.
6. Harding, H.P., et al. 2003. An integrated stress response regulates amino acid metabolism and resistance to oxidative stress. *Mol. Cell.* **11**:619–633.
7. Elefteriou, F., et al. 2006. ATF4 mediation of NF1 functions in osteoblast reveals a nutritional basis for congenital skeletal dysplasiae. *Cell Metab.* **4**:441–451.
8. Teitelbaum, S.L., and Ross, F.P. 2003. Genetic regulation of osteoclast development and function. *Nat. Rev. Genet.* **4**:638–679.
9. Elefteriou, F., et al. 2005. Leptin regulation of bone resorption by the sympathetic nervous system and CART. *Nature.* **434**:514–520.
10. Lee, N.K., et al. 2007. Endocrine regulation of energy metabolism by the skeleton. *Cell.* **130**:456–469.
11. Ferron, M., Hinoi, E., Karsenty, G., and Ducy, P. 2008. Osteocalcin differentially regulates beta cell and adipocyte gene expression and affects the development of metabolic diseases in wild-type

mice. *Proc. Natl. Acad. Sci. U. S. A.* **105**:5266–5270.
12. Hinoi, E., et al. 2008. The sympathetic tone mediates leptin's inhibition of insulin secretion by modulating osteocalcin bioactivity. *J. Cell Biol.* **183**:1235–1242.
13. Delépine, M., et al. 2000. EIF2AK3, encoding translation initiation factor 2-alpha kinase 3, is mutated in patients with Wolcott-Rallison syndrome. *Nat. Genet.* **25**:406–409.
14. Harding, H.P., et al. 2001. Diabetes mellitus and exocrine pancreatic dysfunction in perk$^{-/-}$ mice reveals a role for translational control in secretory cell survival. *Mol. Cell.* **7**:1153–1163.
15. Scheuner, D., et al. 2001. Translational control is required for the unfolded protein response and in vivo glucose homeostasis. *Mol. Cell.* **7**:1165–1176.
16. Ron, D., and Walter, P. 2007. Signal integration in the endoplasmic reticulum unfolded protein response. *Nat. Rev. Mol. Cell Biol.* **8**:519–529.
17. Oyadomari, S., Harding, H.P., Zhang, Y., Oyadomari, M., and Ron, D. 2008. Dephosphorylation of translation initiation factor 2alpha enhances glucose tolerance and attenuates hepatosteatosis in mice. *Cell Metab.* **7**:520–532.
18. Yadav, V.K., et al. 2008. Lrp5 controls bone formation by inhibiting serotonin synthesis in the duodenum: an entero-bone endocrine axis. *Cell.* **135**:825–837.
19. Unger, R.H. 1985. Glucagon physiology and pathophysiology in the light of new advances. *Diabetologia.* **28**:574–578.
20. Puigserver, P., et al. 2003. Insulin-regulated hepatic gluconeogenesis through FOXO1-PGC-1alpha interaction. *Nature.* **423**:550–555.
21. Granner, D., Andreone, T., Sasaki, K., and Beale, E. 1983. Inhibition of transcription of the phosphoenolpyruvate carboxykinase gene by insulin. *Nature.* **305**:549–551.
22. Dickens, M., Svitek, C.A., Culbert, A.A., O'Brien, R.M., and Tavare, J.M. 1998. Central role for phosphatidylinositide 3-kinase in the repression of glucose-6-phosphatase gene transcription by insulin. *J. Biol. Chem.* **273**:20144–20149.
23. Wolfrum, C., Asilmaz, E., Luca, E., Friedman, J.M., and Stoffel, M. 2004. Foxa2 regulates lipid metabolism and ketogenesis in the liver during fasting and in diabetes. *Nature.* **432**:1027–1032.
24. Iynedjian, P.B., et al. 1989. Differential expression and regulation of the glucokinase gene in liver and islets of Langerhans. *Proc. Natl. Acad. Sci. U. S. A.* **86**:7838–7842.
25. Huang, B., Wu, P., Bowker-Kinley, M.M., and Harris, R.A. 2002. Regulation of pyruvate dehydrogenase kinase expression by peroxisome proliferator–activated receptor- ligands, glucocorticoids, and insulin. *Diabetes.* **51**:276–283.
26. Taniguchi, C.M., Emanuelli, B., and Kahn, C.R. 2006. Critical nodes in signaling pathways: insights into insulin action. *Nat. Rev. Mol. Cell Biol.* **7**:85–96.
27. Tolwani, R.J., et al. 2005. Medium-chain acyl-CoA dehydrogenase deficiency in gene-targeted mice. *PLoS Genet.* **1**:e23.
28. Tontonoz, P., and Spiegelman, B.M. 2008. Fat and beyond: the diverse biology of PPARgamma. *Annu. Rev. Biochem.* **77**:289–312.
29. Rane, S.G., et al. 1999. Loss of Cdk4 expression causes insulin-deficient diabetes and Cdk4 activation results in beta-islet cell hyperplasia. *Nat. Genet.* **22**:44–52.
30. Dacquin, R., Starbuck, M., Schinke, T., and Karsenty, G. 2002. Mouse alpha1(I)-collagen promoter is the best known promoter to drive efficient Cre recombinase expression in osteoblast. *Dev. Dyn.* **224**:245–251.
31. Price, P.A., and Kaneda, Y. 1987. Vitamin K counteracts the effect of warfarin in liver but not in bone. *Thromb. Res.* **46**:121–131.
32. Mantamadiotis, T., et al. 2002. Disruption of CREB function in brain leads to neurodegeneration. *Nat. Genet.* **31**:47–54.
33. Dacquin, R., et al. 2004. Knock-in nuclear localized beta-galactosidase reveals that the tyrosine phosphatase Ptprv is specifically expressed in cells of the bone collar. *Dev. Dyn.* **229**:826–834.
34. Ueki, K., et al. 2000. Restored insulin-sensitivity in IRS-1-deficient mice treated by adenovirus-mediated gene therapy. *J. Clin. Invest.* **105**:1437–1445.